

In Vitro and In Vivo Analyses Reveal Tumor-Derived Exosome miR-558 Promotes Angiogenesis in Tongue Squamous Cell Carcinoma by Targeting Heparinase

Technology in Cancer Research & Treatment
Volume 23: 1-12
© The Author(s) 2024
Article reuse guidelines:
sagepub.com/journals-permissions
DOI: 10.1177/15330338241261615
journals.sagepub.com/home/tct



Bixiao Ding, MS^{1,2}, Qingwen Chen, MS³ , Zhen Wu, MS⁴,
Xiaoguang Li, MD^{5,6}, Yuancheng Ding, MS^{1,2}, Qiong Wu, MS^{1,2},
Liang Han, MD³, and Hao Wu, MD¹

Abstract

This study aimed to investigate the role of miR-558 in tumor angiogenesis by targeting heparinase (HPSE) in tongue squamous cell carcinoma (TSCC)-derived exosomes. In the present study, the role of exosome miR-558 in angiogenesis in vitro and in vivo was investigated by cell proliferation, migration, tube formation, subcutaneous tumor formation in mice, and in vivo Matrigel plug assay. The target genes of miR-558 were detected by means of dual luciferase assay. It was found that TSCC cells secrete miR-558 into the extracellular environment, with exosome as the carrier. Human umbilical vein endothelial cells (HUVEC) ingested exosomes, which not only increased the expression level of miR-558, but also enhanced their proliferation, migration, and tube formation functions. In vivo Matrigel plug assay demonstrated that TSCC cell-derived exosome miR-558 promoted neovascularization in vivo. Compared with negative control cells, TSCC cells over-expressing miR-558 formed subcutaneous tumors in nude mice, with larger volume, heavier mass, and more vascularization. Dual luciferase assay confirmed that HPSE was the direct target gene regulated by miR-558. HPSE promoted the proliferation, migration, and tube formation of HUVECs, and the knockout of HPSE could downregulate the pro-angiogenic effect of miR-558. In summary, miR-558 in TSCC exosomes promotes the proliferation, migration, and tube formation of HUVECs by targeting HPSE, and enhancing tumor angiogenesis.

Keywords

tongue squamous cell carcinoma, exosomes, miR-558, HPSE, angiogenesis

Abbreviations

BCA, bicinchoninic acid; cDNA, complementary deoxyribo nucleic acid; CCK-8, cell-counting kit-8; CM, culture medium; DAPI, 4',6-diamidino-2-phenylindole; DEPC, diethylpyrocarbonate; EDTA, ethylene diamine tetraacetic acid; FBS, fetal bovine serum; FDA, Food and Drug Administration; HPSE, heparinase; miRNA, micro deoxyribo nucleic acid; MMP, matrix metalloprotein; NTA, nanoparticle tracking analysis; OD, optical density; OE, over expression; OSCC, oral squamous cell carcinoma; PBS,

¹ Department of Otolaryngology-Head and Neck Surgery, Affiliated Hospital of Nantong University, Nantong, China

² Nantong University, Nantong, China

³ Department of Otolaryngology-Head and Neck Surgery, Affiliated Tumor Hospital of Nantong University, Nantong, China

⁴ Department of Otolaryngology-Head and Neck Surgery, Changshu Second People's Hospital, Suzhou, China

⁵ Department of Otolaryngology-Head and Neck Surgery, Shanghai Ninth People's Hospital, Shanghai Jiao Tong University School of Medicine, Shanghai, China

⁶ Ear Institute, Shanghai Jiao Tong University School of Medicine; Shanghai Key Lab, Shanghai, China

Bixiao Ding and Qingwen Chen contributed equally to this work.

Corresponding Authors:

Hao Wu, Department of Otolaryngology-Head and Neck Surgery, Affiliated Hospital of Nantong University, Nantong 226000, China.

Email: entwuhao@163.com

Liang Han, Department of Otolaryngology-Head and Neck Surgery, Affiliated Tumor Hospital of Nantong University, Nantong 226361, China.

Email: hl61697@126.com



Creative Commons Non Commercial CC BY-NC: This article is distributed under the terms of the Creative Commons Attribution-NonCommercial 4.0 License (<https://creativecommons.org/licenses/by-nc/4.0/>) which permits non-commercial use, reproduction and distribution of the work without further permission provided the original work is attributed as specified on the SAGE and Open Access page (<https://us.sagepub.com/en-us/nam/open-access-at-sage>).

phosphate buffer saline; PMSF, phenyl methane sulfonyl fluoride; qRT-PCR, quantitative real-time polymerase chain reaction; siRNA, small interfering ribonucleic acid; SDS, sodium dodecyl sulfate; TBS, tris buffered saline; TSCC, tongue squamous cell carcinoma; 5'UTR, 5' untranslated regions; VEGF, vascular endothelial growth factor.

Received: February 14, 2024; Revised: May 16, 2024; Accepted: May 21, 2024.

Research Highlights

1. miR-558 can be secreted by TSCC cells and delivered to HUVECs.
2. miR-558 enhanced angiogenesis in TSCC tumors.
3. miR-558 directly regulates the expression of HPSE in HUVECs.

Introduction

Head and neck squamous cell carcinoma (HNSCC) is a common malignant tumor. According to a global cancer report in 2018, there were 890,000 new cases of HNSCC and 450,000 deaths annually.¹ Tongue squamous cell carcinoma (TSCC) is a relatively common HNSCC, accounting for about 41% of oral and maxillo-facial malignant tumors.² Prone to early metastasis, the local and regional recurrence rates of TSCC are 23.9% and 20.4%, respectively, and its 5-year survival rate is 50.6%.³ In recent years, some progress has been made in the surgery, radiotherapy, chemotherapy, and immunotherapy of TSCC.⁴⁻⁶ However, the overall survival rate of patients with locally advanced tumors and cervical lymph node metastasis remains low.⁷ For patients who receive radical surgery, major surgical trauma can cause damage to swallowing, speech, and even breathing functions, leading to a severe decline in quality of life.

We detected and identified circRNA in fresh TSCC tissue samples through high-throughput sequencing in the early stage. Subsequent experiments confirmed that hsa_circ_0000231 was highly expressed in TSCC tumor tissue, and promoted the proliferation, migration, and invasion of TSCC cells through the Wnt/ β -catenin signaling pathway.⁸ Through online prediction websites Target-Scan and miRanda, we discovered that miR-558 might be one of the candidate miRNAs adsorbed by hsa_circ_0000231,⁹ and the downstream molecule miR-558 was related to the occurrence and development of tumor. Through a differential analysis of miRNA chips of TSCC tissues in the NCBI database (GSE28100), we found that miR-558 was highly expressed in human TSCC tissues. Through literature search, it was found that in bladder cancer, miR-558 can improve the proliferation, migration, and invasion abilities of tumor cells, and the supernatant of tumor cell lines can promote angiogenesis, but in-depth mechanism research is lacking.¹⁰ Not only tumor angiogenesis provides the nutrients needed for its growth, but also pathological angiogenesis is probably an important factor that promotes distant tumor metastasis.¹¹ It has been reported that heparinase (HPSE) protein also promotes neovascularization, thus accelerating the progression of malignant tumors.¹² Accordingly, we carried out research on whether miR-558 from TSCC-derived exosomes promoted tumor angiogenesis in tumor microenvironment, and whether it was related to HPSE.

Materials and Methods

Isolation, Characterization, and Quantification of Exosome

TSCC cell lines Tca-8113 and SCC-25 were cultured in serum-free medium for 48 h, and the supernatant was collected and centrifuged at a low speed with differential gradients, that is, 300 r/min for 10 min, 2000 r/min for 30 min, and 10,000 r/min for 1 h. The precipitate was discarded, the cell supernatant after differential centrifugation was placed in a ultracentrifuge, and ultracentrifuged at a speed of 54,000 r/min for 2 h. All centrifugation procedures were carried out at 4 °C, and the precipitate was resuspended in phosphate buffer saline (PBS) solution. After the exosome suspension was diluted with PBS, the particle size of exosome was analyzed by a ZetaView particle size analyzer. The exosomes were lysed with Radio Immunoprecipitation Assay (RIPA) and exosome protein was extracted, the concentration of exosome protein was measured with a BCA kit, and the surface proteins CD9 and CD63 of exosome were identified by means of western blot. The exosome suspension was placed under a transmission electron microscope (HT7800, JPN) to observe its microscopic morphology.

Cell Culture

The human umbilical vein endothelial cells (HUVEC) was donated by the Clinical Experimental Center of the Affiliated Hospital of Nantong University and cultured in RPMI-1640 medium containing 15% fetal bovine serum (FBS). Human oral keratinocytes (HOK) and TSCC cell lines (CAL27, Tca-8113, and SCC-25) were donated by the Department of Head and Neck Surgery, the Ninth People's Hospital of Shanghai Jiaotong University. SCC-25 cells were cultured in DMEM/F12 medium containing 10% fetal bovine serum (FBS). CAL27 and HOK cells were cultured in DMEM high glucose medium containing 10% FBS. Tca-8113 cells were cultured in 1640 medium containing 10% FBS.

Extracellular Vesicle Track Experiment

The PKH26 working solution was configured lucifugally, and the exosomes of Tca-8113 and SCC-25 were incubated with PKH26 working solution in darkness for 20 min. The exosomes stained by fluorescence were incubated using HUVEC lucifugally for 24 h. HUVEC cells were fixed with 4% paraformaldehyde for 20 min, and then stained with DAPI for 10 min. Images were obtained under an inverted microscope (OLYMPUS, JPN) and the images were synthesized by ImageJ software.

RNA Oligonucleotides, Plasmids, and Virus

The following materials were synthesized by Genechem (Shanghai, China): lentiviral vectors expressing miR-558 (OE-miR-558) and their control (OE-NC), anti-miR-558 and its control (anti-NC). According to the instructions, the cells were plated in six-well plates and transfected. After 24 h, the virus-containing supernatant was discarded, antibiotic-free medium was added, and further incubated in a 5% CO₂ incubator at 37 °C. After three passages, the medium containing puromycin was added to select stable strains. The plasmids of the overexpressing HPSE and control group were synthesized by Genechem Shanghai, China. HUVEC was plated in a six-well plate, 2 mL opti-MEM low-serum medium was added, 4 µg plasmid was dissolved in 250 µL opti-MEM low-serum medium, 10 µL Lipofectamine 2000 was added to opti-MEM low-serum medium, plasmid mixed with Lipofectamine 2000 was added to HUVEC medium, and the cell supernatant was discarded after 6 h, and further experiments were carried out after culturing for 24 h.

Small-interfering RNAs (siRNAs) of HPSE together with their negative control were synthesized with Ribobio (Guangzhou, China): siRNA-1, 5'-CTAACAGTTTCCTTAAGAA-3'; siRNA-2, 5'-GAAGGAAGCTTCGAGTATA-3'; siRNA-3, 5'-CCATAAACCTCCATAATGT-3'. 100 pmol siRNA was dissolved in 250 µL opti-MEM low-serum medium, 5 µL Lipofectamine 2000 was added to opti-MEM low-serum medium, and the plasmid was mixed with Lipofectamine 2000 and then added to HUVEC medium. After 6 h, the supernatant was abandoned and cultured for 24 h.

RNA Isolation, PCR

The cells and exosomes were lysed with TRIzol reagent, and cel-miR-39-3p was added to the exosome mixture before chloroform was added. Total RNA was extracted and dissolved in diethylpyrocarbonate water. The concentration of RNA was determined through a Nanodropone ultraviolet spectrophotometer. RT-PCR assay was done with a ThermoFisher K1622 reverse transcription kit to reverse transcribed RNA into cDNA for further study. cel-miR-39-3p was used as an exogenous reference for cellular exosomes and RNU6 was used as an endogenous reference for cell samples. qRT-PCR was done with a Ribobio primer kit. The primers of miRNAs or mRNAs used in this study were as follows: miR-558 was synthesized by Ribobio (Guangzhou, China); miR-39-3p (Forward: 5'-TCACCGGGTG TAAATCAGCTTG-3'); RNU6 (Forward: 5'-CTCGCTTCGG CAGCACA-3'); GAPDH (Forward: 5'-GTCTCCTCTGACTT CAACAGCG-3'; Reverse: 5'-ACCACCCTGTTGCTGTAGCC AA-3'); HPSE (Forward: 5'-CCATAAACCTCCATAATGT CACC-3', Reverse: 5'-CACCATCTTTAGAGTTAGACC ATTG-3'). Set up the real-time fluorescent quantitative PCR instrument according to the instructions of the primer kit, and record the experimental results.

Western Blot

Cells and exosomes were lysed with RIPA, the total protein was extracted, and the protein concentration was determined by a

BCA kit. The protein was dissolved in a 5× protein loading buffer at a ratio of 1:4. 10% SDS-PAGE was used to separate proteins by electrophoresis at a constant voltage of 100 V, and proteins were printed onto PVDF membrane at 4 °C with a constant current of 300 mA. Primary antibodies, including anti-matrix metalloproteinase 9 (MMP9), anti-heparanase (HPSE; 1:1000; Proteintech), anti-glyceraldehyde-3-phosphate dehydrogenase (GAPDH; 1:1000; Sangon Biotech), and anti-vascular endothelial growth factor A (VEGF-A; 1:1000; ABclonal) antibodies, Primary antibody was used to incubate overnight and the membrane was washed with TBST solution for three times, 10 min each time. After the HRP-conjugated secondary antibody (1:1000; Sangon Biotech) was incubated for 1 h, the membrane containing separated proteins was washed with TBST solution for 3 times, 5 min each time. With GAPDH as the internal reference protein, the image of protein band was captured by Gel Imager (Gel Doc XR, USA).

Cell Proliferation Assay

The cells in logarithmic growth phase were digested and the centrifuged cells were re-suspended in medium. 2500 cells were added to each well of a 96-well plate, 10 µL of Cell Counting Kit 8 (CCK8, Genomeditech) was added to each experimental well for 3 days in a row, and the OD value of the well was measured by a multifunctional microplate reader (Thermofisher, USA) after incubating in the dark for 3 h.

Cell Migration Assay

The cells in the logarithmic growth phase were digested, the HUVEC content was diluted to 1.5×10^5 /mL, and the tumor cell content was diluted to 5×10^5 /mL. The 24-well plate was placed in a small chamber, 200 µL cell suspension was added to the upper chamber, and 600 µL medium containing 10% FBS was added to the lower chamber to ensure chemotaxis of the solution in the lower chamber. The chambers in the HUVEC group were recovered after 24 h, while the chambers in the tumor cell group were recovered after 36 h. Cells were fixed with paraformaldehyde for 20 min and stained with crystal violet (Solarbio, Beijing, China) for 10 min. The cells in the upper chamber were wiped off with a cotton swab, and the small chamber was washed with PBS solution and let dry. Pictures were taken under a microscope (OLYMPUS, JPN).

Tube Formation Assay

50 µL of Matrigel (model: BD356234) was spread on the bottom of the precooled 96-well plate at 4 °C using a precooled pipette tip and placed at 37 °C for 1 h. HUVEC cells were suspended in serum-free medium after the Matrigel was solidified. 1.5×10^4 HUVEC cells were added to each well, and placed in a cell incubator for 6 h, observed and photographed under an inverted microscope.

Luciferase Reporter Assay

Dual luciferase reporter plasmids and miR-558 mimics were designed by Limbio. With Lipofectamine 2000 transfection reagent (Invitrogen, USA), HUVECs were co-transfected with the reporter plasmid of the luciferase vector containing the promoter sequence of HPSE and miR-558 mimics or NC. After 48 h of incubation, cell lysates were collected and added to a 96-well plate, and the wavelength of luciferase was detected by a microplate reader (Thermofisher, USA).

In Vivo Matrigel Plug Assay

500 μ L of low growth factor Matrigel (BD: 356231) was mixed with exosomes from Tca-8113 and SCC-25 cells and injected into the right shoulder of c57BL/6 mice with a needle gauge of 1 cm. 10 days later, the Matrigel plug was removed and stored in 4% paraformaldehyde. With the help of paraffin section and immunohistochemical staining techniques, we can stain CD31 molecule in the Matrigel plug and evaluate the internal vascular density. The nude mice were euthanized via intravenous administration of sodium pentobarbital, and the carcass was securely sealed and dispatched to the animal center for centralized and safe disposal (The Tab of Animal Experimental Ethical Inspection, No.S20210130-906).

Animal Model

TSCC tumor cells in the logarithmic growth phase were digested into single-cell suspension and injected into the right armpit of 5-week-old nude mice, with 5 mice in each group ($n=5$). After 14 days, fresh subcutaneous tumors were taken out and the weight of tumors was accurately measured with an electronic scale. The longest diameter (a) and the shortest diameter (b) of tumors were accurately measured with a vernier caliper. The approximate volume of tumors was estimated through the formula $V = a \times b^2 / 2$. The removed tumor tissues were sectioned and used for immunohistochemical staining experiment.

Statistical Analysis

Statistical analysis was performed using GraphPad Prism 8.3 statistical software. The comparison between two groups was done with an unpaired Student's t-test. The comparison between three or more groups was done with a one-way ANOVA test.¹³ Statistical results with $*P < 0.05$, $**P < 0.01$, $***P < 0.001$, or $****P < 0.0001$ were considered to be statistically significant.

Results

TSCC Cell-Derived Exosomes Promoted HUVEC Proliferation

Related studies have shown that overexpression of miR-558 cancer cell supernatant can promote HUVEC tube formation.

In order to explore the expression level of miR-558 in TSCC cell lines, we selected HOK, Tca-8113, CAL27, SCC-25 cell lines, and qRT-PCR experiments indicated that the expressions of miR-558 in Tca-8113 and SCC-25 cells in wild-type TSCC cell lines were relatively low (Figure 1A). Ultracentrifugation method was employed to obtain the supernatant precipitate of wild-type TSCC cells, and the nanoparticle tracking (NTA) technology was adopted to prove that the particle size range of the precipitate obtained was between 30 and 150 nm (Figure 1B). The total protein was extracted by Western blot experiment. It was found that the expression levels of CD9 and CD63 proteins in the total protein were much higher than the total protein of cancer cells, and the expressions of protein were consistent with the characteristics of exosomes (Figure 1C). The extracted exosomes showed typical cup-packed and spherical morphology under a transmission electron microscope (Figure 1D).

In an effort to study the biological function of TSCC exosomes on HUVEC, we co-incubated the exosomes of wild-type SCC-25 and Tca-8113 cell lines with HUVEC in a 96-well plate. CCK8 experiment showed that 10 and 100 μ g/mL exosomes played a better role in promoting HUVEC proliferation at 48 and 72 h than those of the control group mixed with PBS.

Comparing the effects of exocrine at different concentrations on HUVEC proliferation, exosomes with a final concentration of 100 μ g/mL had the best proliferation effect at 48 and 72 h. However, the proliferation effect of HUVEC was not further enhanced by co-incubating with 500 μ g/mL exosome suspension (Figure 1E). The above experiments proved that exosomes from Tca-8113 and SCC-25 cell lines can promote the proliferation of HUVECs. Under the conditions of this experiment, TSCC cell-derived exosomes did not show a concentration-dependent effect on the proliferation of HUVECs. We took 100 μ g/mL as the optimal concentration under the experimental conditions.

TSCC Exosomal miR-558 Promoted the Proliferation, Migration, and Tube Formation of HUVEC In Vitro

To determine the function of exosome miR-558 in TSCC angiogenesis, we first built Tca-8113 and SCC-25 cell lines that stably overexpressed miR-558, to obtain exosomes with high expression of miR-558. Then the total RNA of cancer cells and exosomes with stable overexpression of miR-558 and its negative control group were extracted, and the expression of miR-558 was determined by qRT-PCR. The results showed that overexpression of miR-558 lentivirus increased the expression of miR-558 in cells and exosomes (Figure 2A).

After incubating HUVECs with TSCC cell supernatants, the HUVECs incubated with the supernatants of Tca-8113 and SCC-25 cell lines that overexpressed miR-558 had stronger proliferation ability than the control group, the number of migrating cells increased, and the tubes generated were markedly increased (Supplemental Figure 1A–D). To further investigate whether the above results were associated with exosomes, we used exosomes from Tca-8113 and SCC-25 cell lines that

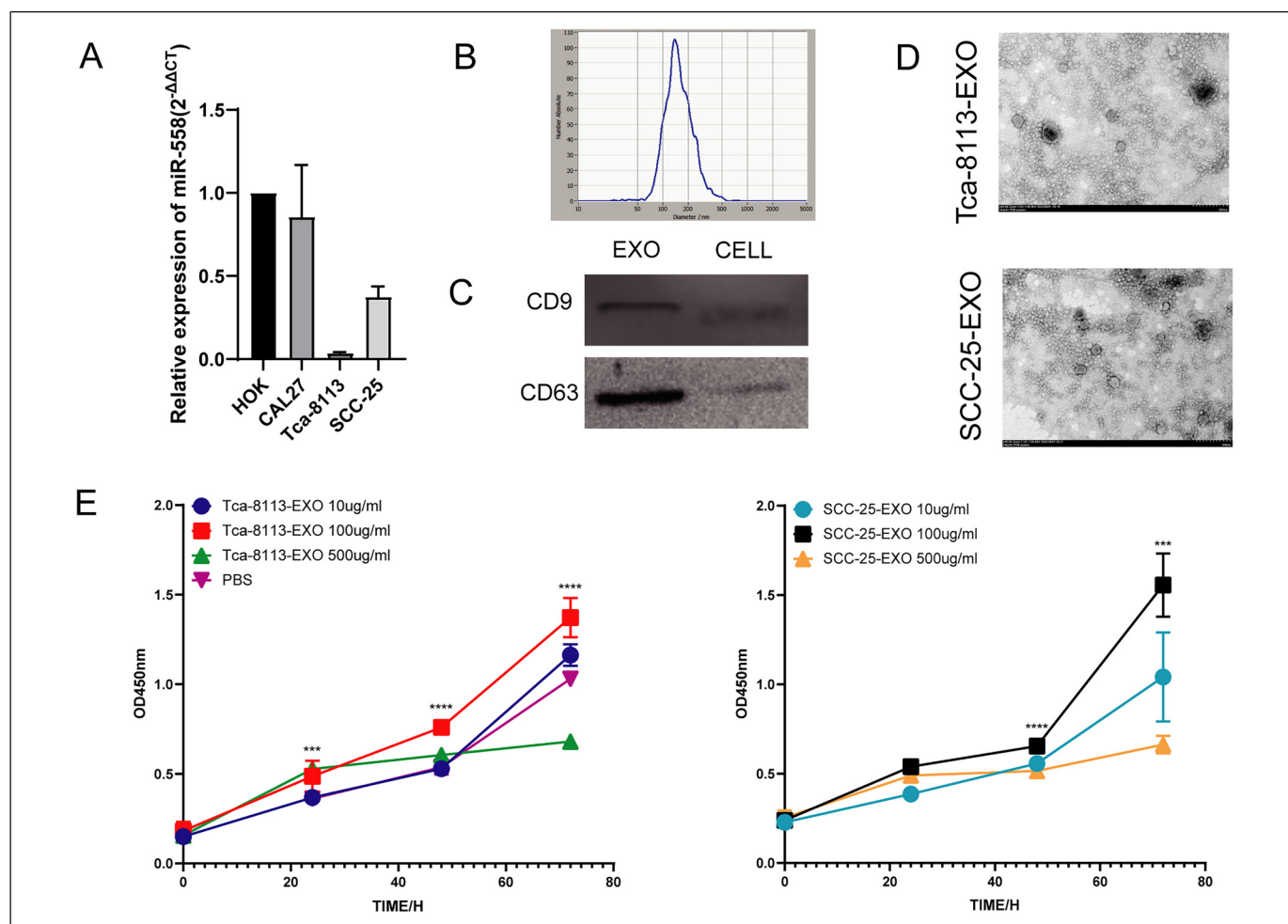


Figure 1. Wild-type TSCC exosomes regulate HUVECs proliferation. (A) The expression level of miR-558 in HOK, CAL27, Tca-8113, and SCC-25 cells was detected by qRT-PCR. (B) The particle size distribution of extracted exosomes was detected by nanoscale particle size analyzer. (C) The expression levels of CD9 and CD63 were detected by western blot. (D) Morphology of exosomes in Tca-8113 and SCC-25 cells under transmission electron microscopy. (E) HUVECs proliferation curves of wild-type Tca-8113 and CAL27 exosomes after incubation with HUVECs. EXO, exosomes. * $P < 0.05$, ** $P < 0.01$, *** $P < 0.001$, **** $P < 0.0001$.

overexpressed miR-558 to incubate with HUVECs, and the HUVECs after incubation showed stronger proliferation ability than the negative control group. The number of migrated cells was larger than that of the negative control group, and the number of tubes was greater (Figure 2B and D).

Anti-miR-558 lentivirus and its NC virus were transfected into HUVEC, and the treated cells were incubated with the exosomes of cancer cells overexpressing miR-558 for 24 h. The experimental results indicated that pre-transfection of anti-miR-558 could antagonize the promoting effect of exosomes overexpressing miR-558 on HUVEC proliferation, migration, and tube formation (Figure 2B–D).

In order to further determine the direct effect of miR-558 on HUVEC, we directly transfected HUVEC with lentivirus overexpressing miR-558 and repeated the above experiment. The transfection of lentivirus raised the expression level of miR-558 in HUVEC (Figure 2A), and the upregulation of

miR-558 improved HUVEC proliferation, migration, and tube formation (Supplemental Figure 2B–D).

miR-558 Was Delivered to HUVEC from TSCC Cell Lines by Exosomes

We speculated that TSCC-derived exosomal miR-558 was delivered into HUVECs to initiate TSCC-associated angiogenesis. Thus, after we incubated the exosomes of TSCC cells in the overexpression miR-558 group and its negative control group with HUVECs, qRT-PCR showed that the expression of miR-558 in HUVEC cells in the experimental group was heightened (Figure 3A and B). The extracellular vesicle track experiment captured the fluorescent images of the uptake of PKH26-stained exosomes by HUVECs. The images of three different colors were fused with ImageJ software

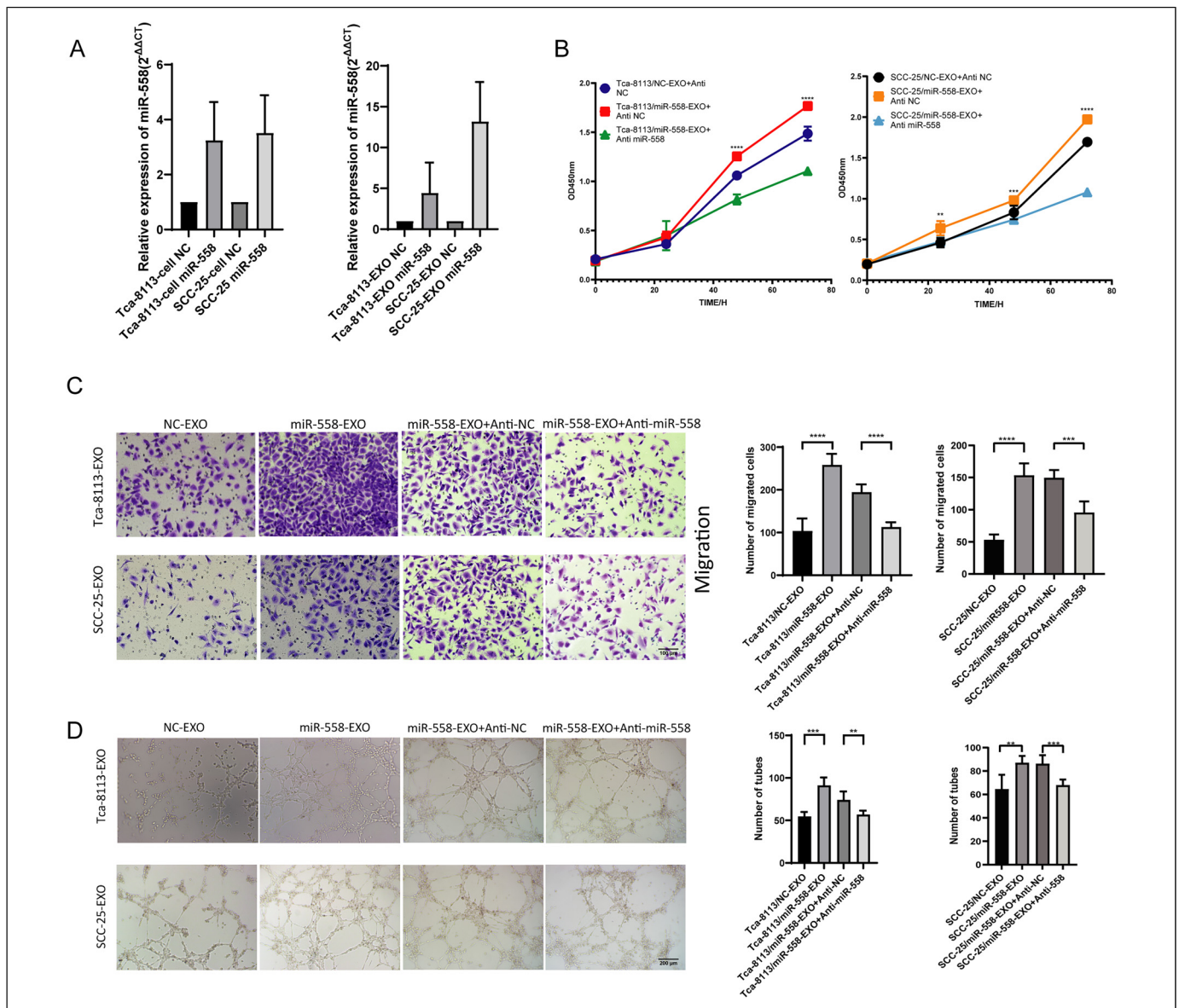


Figure 2. TSCC-derived exosomes mir-558 promotes the proliferation, migration, and tube formation of HUVECs. (A) qRT-PCR detection of miR-558 expression levels in cancer cells with stable overexpression of miR-558 and negative control cancer cells. The right figure shows the expression levels of miR-558 in exosomes of the corresponding groups. (B) Proliferation curve of HUVECs after treatment with exosomes from cancer cells overexpressing miR-558 and negative control cancer cells. (C) Representative images of HUVECs that spanned to the bottom of the transwell chamber after treatment with exosomes from cancer cells overexpressing miR-558 and negative control cancer cells. The number of migrated cells is shown in the chart on the right. (D) Representative images of tubes formed after treatment of HUVECs with exosomes from cancer cells overexpressing miR-558 and negative control cancer cells, and the number of tubes formed is shown in the right chart. * $P < 0.05$, ** $P < 0.01$, *** $P < 0.001$, **** $P < 0.0001$.

to show that the red fluorescence was distributed within the cell outline and had a clear boundary with blue nucleus (Figure 3C). The above experiments demonstrated that TSCC cell exosomes were successfully taken up by HUVECs.

TSCC Cell Line-Derived Exosomal miR-558-Induced Neovascularization in Vivo

We further explored the function of exosomal miR-558 in neovascularization in vivo. Exosomes were isolated from TSCC

cell supernatants, then mixed with Matrigel and injected into the right shoulder of mice. After 10 days, the Matrigel plug was recovered, and the results indicated that the Matrigel mixed with overexpressed miR-558 had more neovascularization than the control group (Figure 4A and B). Immunohistochemical staining results indicated that Matrigel plugs mixed with exosomes overexpressing miR-558 had more CD31 staining areas than those in the control group, suggesting that Matrigel plugs mixed with exosomes overexpressing miR-558 had higher vascular density (Figure 4C and D). The above in vivo experiments

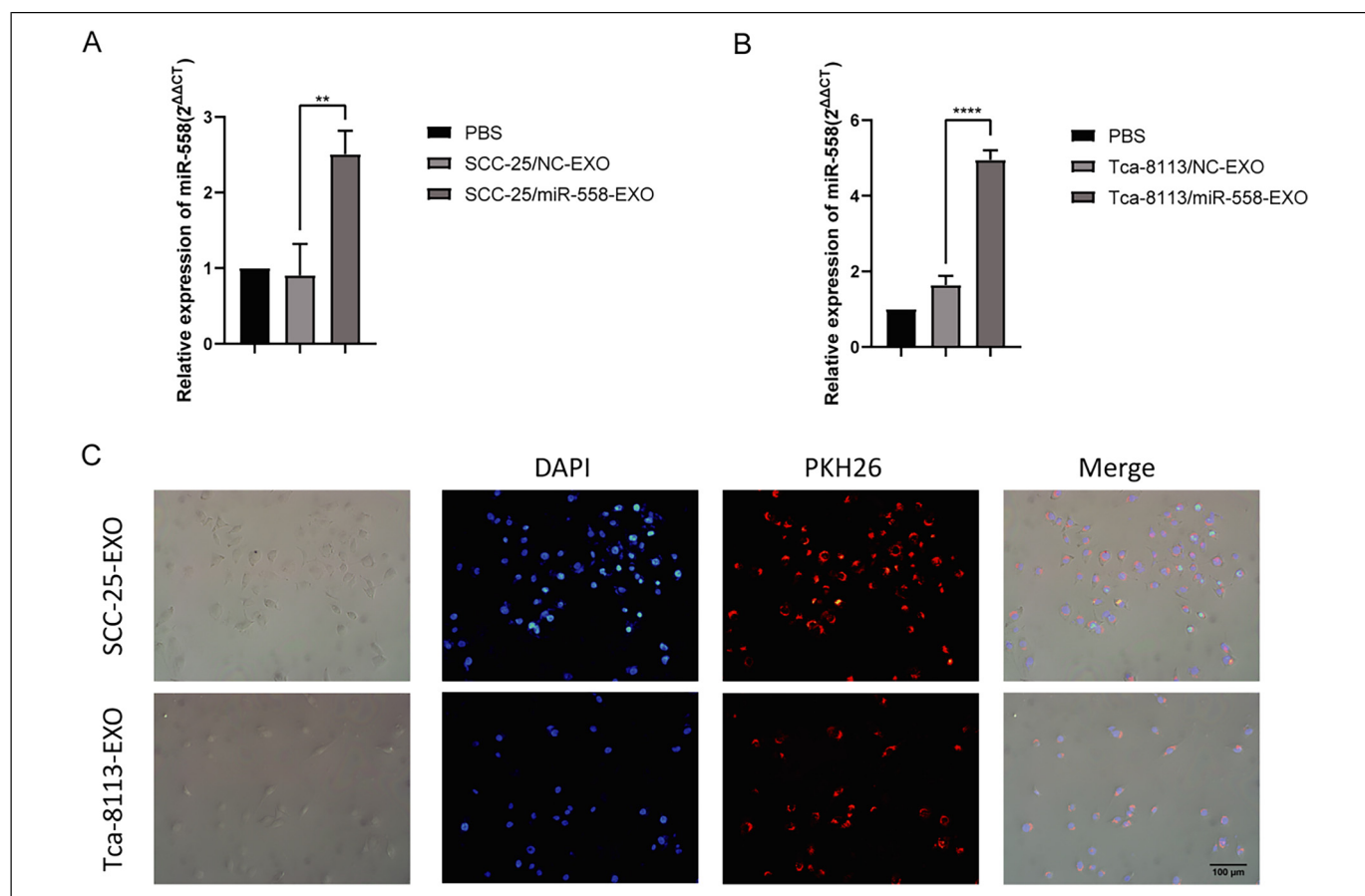


Figure 3. miR-558 is packaged into exosomes and delivered from TSCC cells to HUVECs. (A–B) miR-558 expression level of HUVECs after incubation of TSCC cell-derived exosomes with HUVECs. (C) Fluorescence microscope image of PKH26-stained exosomes of Tca-8113 and SCC-25 cells incubated with HUVECs and DAPI stained HUVECs nuclei.

demonstrated that TSCC-derived exosomal miR-558 had a better pro-angiogenic effect.

miR-558 Promoted Tumor Growth and Increased the Vascular Density of Tumor in Nude Mice

To further investigate whether miR-558 can promote tumorigenesis *in vivo* by inducing neovascularization, we injected Tca-8113 and SCC-25 cells subcutaneously into the right axilla of nude mice, and found that TSCC cells overexpressing miR-558 had larger tumor volume and heavier tumor mass than those in the negative control group (Figure 5A–F). We assessed the number of microvessels in tumor nodules by CD31 staining, and the results showed that the expression of CD31 molecules was upregulated in tumor sections overexpressing miR-558, suggesting a high vascular density in neoplastic tumors (Figure 5G–J). These results showed that miR-558 can promote the growth of TSCC tumors *in vivo* by inducing tumor angiogenesis.

miR-558 Promoted Angiogenesis by Targeting HPSE

In order to further investigate the molecular mechanism how exosomal miR-558 promoted angiogenesis, we designed a dual-

luciferase experiment with reference to information on the sequence of the 5'UTR binding site between miR-558 and HPSE reported in the study of gastric cancer. The results proved that miR-558 can bind to the promoter sequence of the 5'UTR of HPSE. Overexpression of miR-558 in HUVECs increased the promoter luciferase activity of HPSE, which was counteracted by mutation in the binding site sequence (Figure 6A and B). The expression level of HPSE mRNA in HUVEC was verified by qRT-PCR. Compared with the control group, the expression level of HPSE mRNA in HUVEC overexpressing miR-558 increased (Figure 6C). The expressions of miR-558 downstream protein HPSE and HPSE downstream protein MMP9 and VEGF-A were detected by western blot assay. The results showed that compared with the negative control group, the expression of HPSE in HUVEC that overexpressed miR-558 increased, while the expression of VEGF-A and MMP9 regulated by HPSE was significantly upregulated (Figure 6D). The above experiments suggested that the expression of HPSE was regulated by miR-558, but whether it promoted angiogenesis via HPSE remained unclear.

We synthesized the overexpressed HPSE and negative control plasmids. In the experimental group, the HPSE

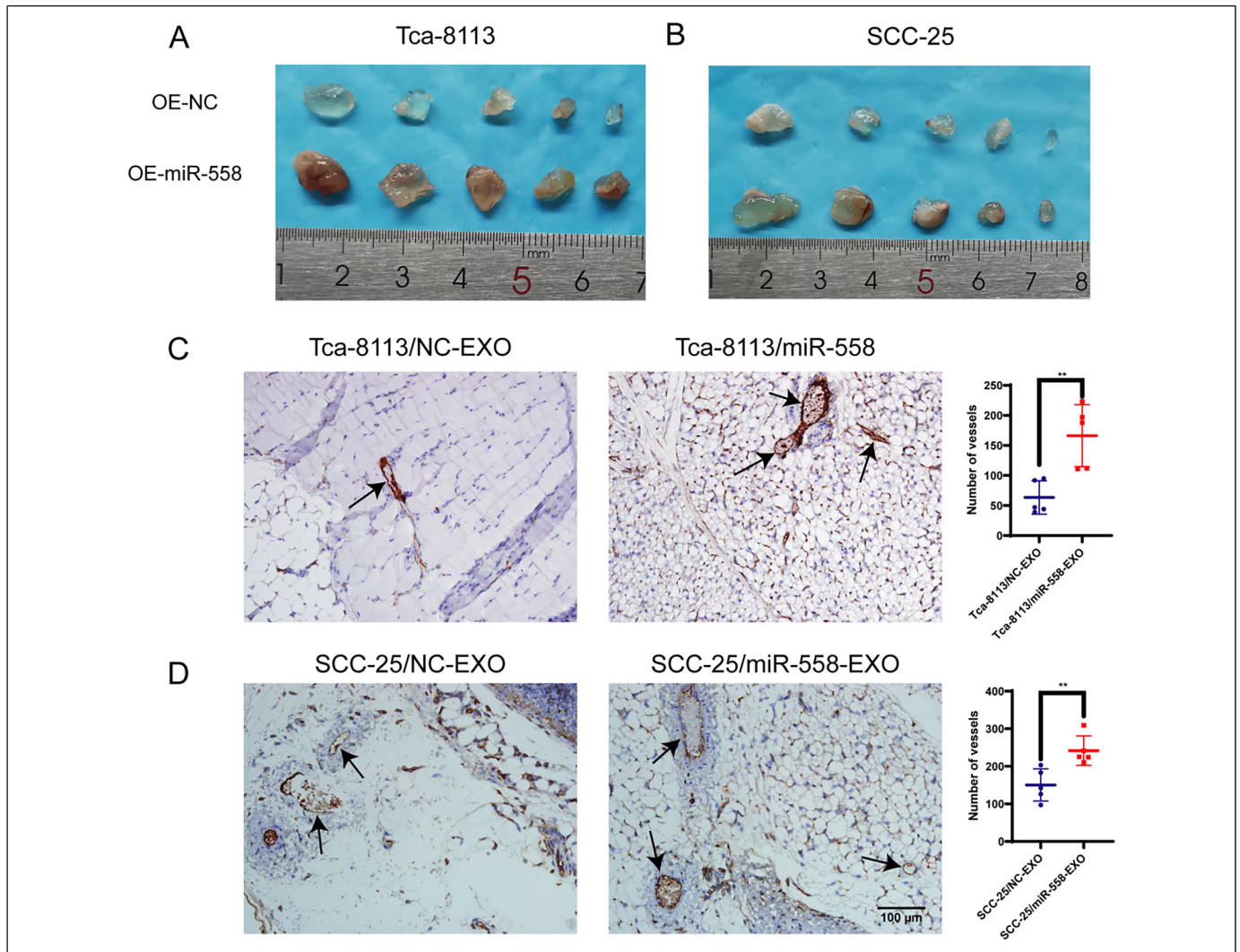


Figure 4. TSCC cell exosomes induce neovascularization in vivo. (A) Images of Matrigel plug formed in mouse axilla after mixing Matrigel with Tca-8113 or SCC-25 cell-derived miR-558-EXO or NC-EXO. (B–C) Representative images of CD31 immunohistochemical staining of paraffin-embedded Matrigel plug sections. The number of CD31-positive microvessels in the Matrigel plug is shown on the right. * $P < 0.05$, ** $P < 0.01$, *** $P < 0.001$, **** $P < 0.0001$.

expression of HUVEC significantly increased (Supplemental Figure 3A), and the overexpression of HPSE can facilitate the proliferation, migration, and tube formation of HUVEC (Supplemental Figure 3B–D). We used three siRNAs to knock out the HPSE gene of HUVEC, and qRT-PCR was used to verify the knockout effect. The results showed that the knockout effect of siRNA-HPSE1 was the best (Figure 6E). Therefore, we selected it for further experiment. We used siRNA-HPSE1 to transfect HUVEC that overexpressed miR-558. The results of CCK8 experiment indicated that HPSE knockout significantly downregulated the effect of miR-558 on the promotion of HUVEC proliferation at 72 h (Figure 6F). The results of Transwell experiment showed that the knockout of HPSE can reverse the promoting effect of miR-558 on HUVEC migration (Figure 6G). The results of tube formation experiment also showed that the knockout of HPSE could downregulate the promoting function of HUVEC

tube formation by overexpressing miR-558 (Figure 6H). The above results indicated that miR-558 promoted the proliferation, migration, and angiogenesis of HUVECs by regulating the expression of HPSE.

Discussion

Malignant tumor cells have strong proliferation ability. During the rapid proliferation, the tumor tissues are in a relatively hypoxic state, which will stimulate tumor cells to secrete pro-angiogenic factors and induce neovascularization in tumor tissues.¹⁴ Neovascularization not only brings oxygen and nutrients into tumor cells, but also raises the pressure of tumor interstitial tissues and facilitates the drainage of interstitial materials into lymph nodes because of its high permeability. This mechanism is often one of the factors that promote tumor metastasis and regional recurrence.¹⁵ It has been reported that

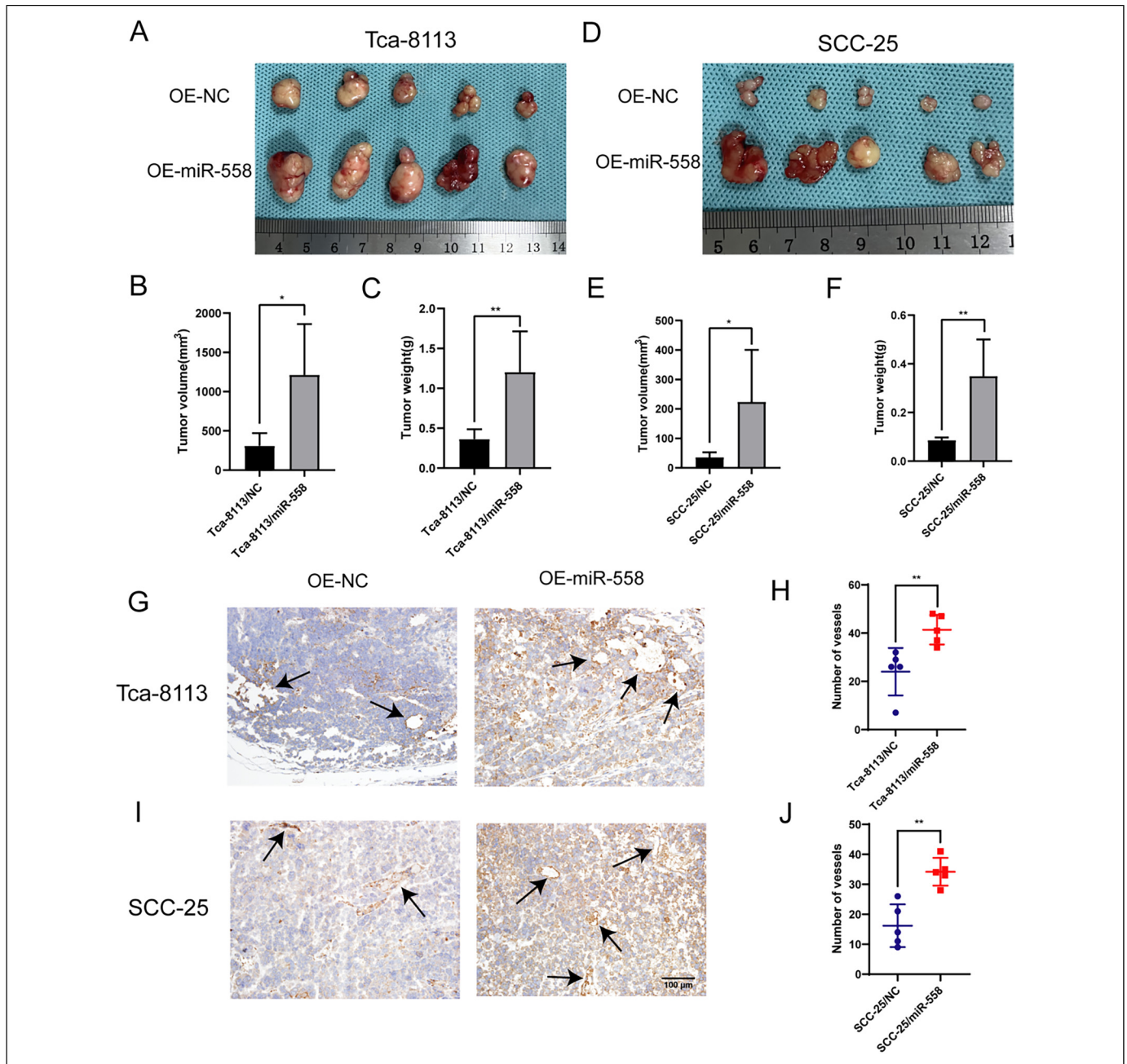


Figure 5. miR-558 promotes malignant progression of TSCC in vivo. (A–C) Tca-8113 cells overexpressing miR-558 produced larger and heavier tumors in nude mice subcutaneously. (D–F) SCC-25 cells overexpressing miR-558 formed larger and heavier tumors in nude mice subcutaneously. (G–H) Representative images of CD31 immunohistochemical staining in paraffin-embedded Tca-8113 tumor sections. The number of CD31-positive microvessels is shown in the chart on the right. (I–J) Representative images of CD31 immunohistochemical staining in paraffin-embedded SCC-25 tumor sections. The number of CD31-positive microvessels is shown in the chart on the right. * $P < 0.05$, ** $P < 0.01$, *** $P < 0.001$, **** $P < 0.0001$.

the expression of angiogenic factors in patients with HNSCC is higher than that in healthy people, which may result in a poor prognosis due to the enhanced tumor resistance to traditional cytotoxic drugs.¹⁶ At present, a variety of targeted drugs have been developed for tumor angiogenesis. Bevacizumab was the first antiangiogenic drug approved by FDA in the United States. By targeting the inhibition of VEGF-A downregulation of angiogenesis, bevacizumab can effectively treat metastatic

rectal cancer, advanced non-small cell lung cancer, ovarian cancer, and other malignant tumors, but the effect is not ideal in HNSCC.¹⁷ Although antiangiogenic targeted drugs, such as sorafenib and sunitinib developed based on tyrosine kinase receptors, showed relatively lower toxicity in HNSCC clinical trials, they did not achieve a marked anticancer effect.¹⁸ Therefore, it is very important to carry out in-depth research on HNSCC and find a more reliable and safe therapeutic target.

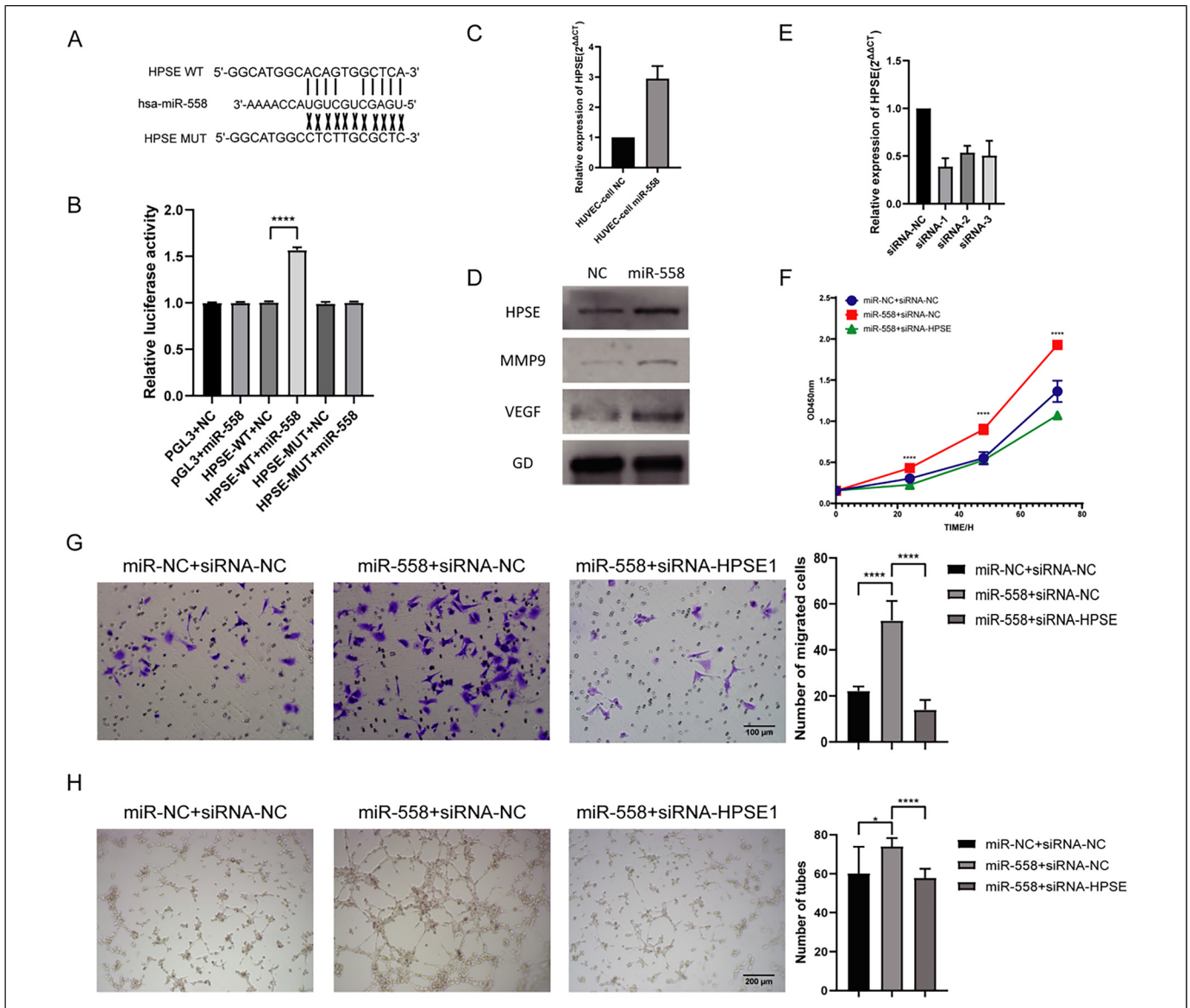


Figure 6. miR-558 regulates HPSE to promote proliferation, migration, and tube formation in HUVECs. (A) Construction of wild-type and mutant luciferase-containing plasmid sequences of predicted binding sites between HPSE and miR-558. (B) Co-transfect HPSE wild-type and mutant luciferase-containing plasmids for the miR-558 binding site in HUVEC cells, as well as miR-558 mimics or NC mimics, and detect the luciferase activity to reflect the binding situation. (C) The expression level of HPSE in HUVECs after overexpression of miR-558 was detected by qRT-PCR. (D) Protein expression of HPSE, VEGF-A and MMP9 in HUVEC after overexpression of miR-558. (E) After transfecting HUVEC with three small interfering RNAs and one control sequence, the expression level of HPSE was detected by qRT-PCR experiment. (F) The effect of knocking out HPSE on the proliferation ability of HUVEC overexpressing miR-558. (G–H) Representative images of migration and tube formation of miR-558-overexpressed HUVECs knocked out of HPSE, the number of migrated cells and the number of tubes are shown in the right chart. * $P < 0.05$, ** $P < 0.01$, *** $P < 0.001$, **** $P < 0.0001$.

In previous studies, our team found that hsa_circ_0000231 was highly expressed in TSCC tumor tissues and promoted the proliferation, migration, and invasion of TSCC cells. At the same time, it was predicted that miR-558 may be one of the candidate molecules regulated by its targeting. Through literature search, miR-558 can promote the occurrence of lung cancer and paclitaxel resistance,¹⁹ and upregulate the transcription of HPSE gene in retinoblastoma.²⁰ The supernatant of bladder cancer cells overexpressing miR-558 has a role in promoting

HUVEC angiogenesis,¹⁰ but what factors in the supernatant play a role in neovascular angiogenesis and whether exosomes play a role as transporters have not been explained, and no relevant studies have been conducted on the role of miR-558 in exosomes in HNSCC. Due to extremely high stability of exosomal miRNA, it can not only be employed as an effective biomarker by expressing the out-of-control miRNA in cancer cells, but also act as a medium to deliver miRNA to target cells and regulate the corresponding functions, when it is secreted by cancer

cells into the internal environment.^{21–24} Therefore, we carried out a study on miR-558 of TSCC-derived exosomes.

In this study, we found that the expression level of miR-558 increased in exosomes of TSCC cells that overexpressed miR-558. Extracellular vesicles track experiments showed that the exosomes of miR-558 were delivered from TSCC cells to HUVEC as an uptake carrier, and the expression level of miR-558 in HUVEC increased. Compared with the control group, the supernatant and exosome of TSCC cells that overexpressed miR-558 showed stronger promotion of HUVEC proliferation, migration, and tube formation, and HUVEC pretreated with anti-miR-558 could downregulate the above results. These results demonstrated the ability of miR-558 to promote angiogenesis in vitro. To further explore the role of TSCC exosome miR-558 in vivo, we performed in vivo Matrigel plug assay and subcutaneous tumor formation experiment on c57BL/6 mice and nude mice, respectively. The results of in vivo Matrigel plug assay showed that Matrigel mixed with exosomes overexpressing miR-558 had a higher density of angiogenesis in mice, and the results of subcutaneous tumor formation experiment indicated that the TSCC cell line overexpressing miR-558 had larger tumor size, heavier weight, and higher density of neovasculum in nude mice.

Based on the prediction that miR-558 probably targeted the regulation of HPSE, we carried out research on HPSE. HPSE is a protein endonuclease secreted by tumor cells, which has the activity of degrading and remodeling extracellular matrix (ECM). Its expression is increased in a variety of malignant tumors. It can promote angiogenesis, degrade the vascular basement membrane, and extracellular matrix, and is an important factor for promoting invasion and metastasis of malignant tumors.¹² HPSE can activate ERK pathway and enhance the expression of matrix metalloproteinase 9 (MMP-9).^{25–27} MMP-9 can raise the concentration of VEGF in tissues and facilitate the binding of VEGF and VEGFR2.^{28,29} In addition, HPSE has been shown to significantly increase the expression of VEGF-An in many cell lines.³⁰ VEGF-A in tumor cells can not only promote tumor angiogenesis, but also enhance vascular permeability. This is probably one of the initiating factors of tumor distant metastasis.^{31,32} In this study, we proved that HPSE was a direct target of miR-558 through dual luciferase experiment. The western blot assay showed that miR-558 promoted the expression of HPSE, MMP-9, and VEGF-An in HUVEC. HPSE overexpressing HUVEC could enhance the proliferation, migration, and tube formation of HUVEC, which proved that HPSE could promote angiogenesis in vitro, and the knockout of HPSE could downregulate the above results. Therefore, we believe that the targeted regulation of HPSE expression by miR-558 is one of the main drivers of angiogenesis.

The study still has certain limitations. Firstly, it is necessary to include multicenter clinical samples of TSCC for comprehensive research purposes. Secondly, additional molecular biology experiments are required to validate the precise mechanism by which miR-558 promotes the proliferation, migration, and angiogenesis of TSCC.

Conclusion

Our study is the first to demonstrate that miR-558 in TSCC-derived exosomes can promote HUVEC proliferation, migration, and tube formation by targeting HPSE, and lead to the formation of tumor neovasculature.

Acknowledgments

All methods were carried out in accordance with relevant guidelines and regulations, and all experimental protocols were approved by Nantong University. All relevant data are within the manuscript and its additional files. The Tab of Animal Experimental Ethical Inspection, No.S20210130-906.


Declaration of Conflicting Interests

The authors declared no potential conflicts of interest with respect to the research, authorship, and/or publication of this article.

Funding

The authors disclosed receipt of the following financial support for the research, authorship, and/or publication of this article: This work was supported by the Postgraduate Research & Practice Innovation of Jiangsu Province #1 (No.SJCX21_1474); Jiangsu Natural Science Foundation #2 (BK20211107); Research Physician Development Fund of Nantong University affiliated hospital #3 (YJXY202204-YSB02); Nantong 226 Talent Project #4 (2020-9); Nantong Science and Technology Project #5 (JCZ2022069, JC2023082); Nantong Health Commission Science and Technology Project #6 (MS2022047, QNZ2023057); Special Project of Clinical Medicine of Nantong University #7 (2022JQ003); Changshu Science and Technology Project #8 (csws20200, cswsq201901).

ORCID iD

Qingwen Chen  <https://orcid.org/0009-0003-4602-4702>

Supplemental Material

Supplemental material for this article is available online.

References

1. Xu Y, Hong M, Kong D, Deng J, Zhong Z, Liang J. Ferroptosis-associated DNA methylation signature predicts overall survival in patients with head and neck squamous cell carcinoma. *BMC Genomics*. 2022;23(1):63.
2. Patel RS, Clark JR, Dirven R, et al. Prognostic factors in the surgical treatment of patients with oral carcinoma. *ANZ J Surg*. 2009;79(1–2):19–22.
3. Caponio VCA, Troiano G, Togni L, et al. Pattern and localization of perineural invasion predict poor survival in oral tongue carcinoma. *Oral Dis*. 2023;29(2):411–422.
4. Colella G, Rauso R, De Cicco D, et al. Clinical management of squamous cell carcinoma of the tongue: Patients not eligible for free flaps, a systematic review of the literature. *Expert Rev Anticancer Ther*. 2021;21(1):9–22.
5. Onidani K, Miura N, Sugiura Y, et al. Possible therapeutic strategy involving the purine synthesis pathway regulated by ITK in tongue squamous cell carcinoma. *Cancers (Basel)*. 2021;13(13):3333.

6. Xi L, Yang Y, Xu Y, et al. The enhanced genomic 6 mA metabolism contributes to the proliferation and migration of TSCC cells. *Int J Oral Sci.* 2022;14(1):11.
7. Chin D, Boyle GM, Porceddu S, Theile DR, Parsons PG, Coman WB. Head and neck cancer: Past, present and future. *Expert Rev Anticancer Ther.* 2006;6(7):1111-1118.
8. Chen QW, Wang DQ, Ding BX, et al. Hsa_circ_0000231 affects the progression of tongue squamous cell carcinoma by activating wnt/ β -catenin signaling pathway. *Zhonghua Er Bi Yan Hou Tou Jing Wai Ke Za Zhi.* 2022;57(10):1230-1239. Chinese.
9. Qiu X, Ke X, Ma H, et al. Profiling and bioinformatics analyses reveal differential expression of circular RNA in tongue cancer revealed by high-throughput sequencing. *J Cell Biochem.* 2019;120(3):4102-4112.
10. Li Y, Zheng F, Xiao X, et al. CircHIPK3 sponges miR-558 to suppress heparanase expression in bladder cancer cells. *EMBO Rep.* 2017;18(9):1646-1659.
11. Lugano R, Ramachandran M, Dimberg A. Tumor angiogenesis: Causes, consequences, challenges and opportunities. *Cell Mol Life Sci.* 2020;77(9):1745-1770.
12. Vreys V, David G. Mammalian heparanase: What is the message? *J Cell Mol Med.* 2007;11(3):427-452.
13. Livak KJ, Schmittgen TD. Analysis of relative gene expression data using real-time quantitative PCR and the 2- $\Delta\Delta C_q$ method. *Methods.* 2001;25(4):402-408.
14. Harris B, Saleem S, Cook N, Searle E. Targeting hypoxia in solid and haematological malignancies. *J Exp Clin Cancer Res.* 2022;41(1):318.
15. Leong SP, Naxerova K, Keller L, Pantel K, Witte M. Molecular mechanisms of cancer metastasis via the lymphatic versus the blood vessels. *Clin Exp Metastasis.* 2022;39(1):159-179.
16. Mineta H, Miura K, Ogino T, et al. Prognostic value of vascular endothelial growth factor (VEGF) in head and neck squamous cell carcinomas. *Br J Cancer.* 2000;83(6):775-781.
17. Argiris A, Li S, Savvides P, et al. Phase III randomized trial of chemotherapy with or without bevacizumab in patients with recurrent or metastatic head and neck cancer. *J Clin Oncol.* 2019;37(34):3266-3274.
18. Hyytiäinen A, Wahbi W, Väyrynen O, et al. Angiogenesis inhibitors for head and neck squamous cell carcinoma treatment: Is there still hope? *Front Oncol.* 2021;11:683570.
19. Li X, Feng Y, Yang B, et al. A novel circular RNA, hsa_circ_0030998 suppresses lung cancer tumorigenesis and taxol resistance by sponging miR-558. *Mol Oncol.* 2021;15(8):2235-2248.
20. Qu H, Zheng L, Pu J, et al. miRNA-558 promotes tumorigenesis and aggressiveness of neuroblastoma cells through activating the transcription of heparanase. *Hum Mol Genet.* 2015;24(9):2539-2551.
21. Boyiadzis M, Whiteside TL. Exosomes in acute myeloid leukemia inhibit hematopoiesis. *Curr Opin Hematol.* 2018;25(4):279-284.
22. Colombo M, Giannandrea D, Lesma E, Basile A, Chiamonte R. Extracellular vesicles enhance multiple myeloma metastatic dissemination. *Int J Mol Sci.* 2019;20(13):3236.
23. Rak J. Extracellular vesicles - biomarkers and effectors of the cellular interactome in cancer. *Front Pharmacol.* 2013;4:21.
24. Zhou W, Fong MY, Min Y, et al. Cancer-secreted miR-105 destroys vascular endothelial barriers to promote metastasis. *Cancer Cell.* 2014;25(4):501-515.
25. Jiang G, Zheng L, Pu J, et al. Small RNAs targeting transcription start site induce heparanase silencing through interference with transcription initiation in human cancer cells. *PLoS One.* 2012;7(2):e31379.
26. Sowmya SV, Rao RS, Prasad K. Prediction of metastasis in oral squamous cell carcinoma through phenotypic evaluation and gene expression of E-cadherin, β -catenin, matrix metalloproteinase-2, and matrix metalloproteinase-9 biomarkers with clinical correlation. *J Carcinog.* 2020;19:8.
27. Yang B, Dong K, Guo P, et al. Identification of key biomarkers and potential molecular mechanisms in oral squamous cell carcinoma by bioinformatics analysis. *J Comput Biol.* 2020;27(1):40-54.
28. Bergers G, Brekken R, McMahon G, et al. Matrix metalloproteinase-9 triggers the angiogenic switch during carcinogenesis. *Nat Cell Biol.* 2000;2(10):737-744.
29. Rodriguez-Manzanique JC, Lane TF, Ortega MA, Hynes RO, Lawler J, Iruela-Arispe ML. Thrombospondin-1 suppresses spontaneous tumor growth and inhibits activation of matrix metalloproteinase-9 and mobilization of vascular endothelial growth factor. *Proc Natl Acad Sci U S A.* 2001;98(22):12485-12490.
30. Cohen-Kaplan V, Naroditsky I, Zetser A, Ilan N, Vlodavsky I, Doweck I. Heparanase induces VEGF C and facilitates tumor lymphangiogenesis. *Int J Cancer.* 2008;123(11):2566-2573.
31. Harney AS, Arwert EN, Entenberg D, et al. Real-Time imaging reveals local, transient vascular permeability, and tumor cell intravasation stimulated by TIE2hi macrophage-derived VEGFA. *Cancer Discov.* 2015;5(9):932-943.
32. Stoletov K, Montel V, Lester RD, Gonias SL, Klemke R. High-resolution imaging of the dynamic tumor cell vascular interface in transparent zebrafish. *Proc Natl Acad Sci U S A.* 2007;104(44):17406-17411.